Hygrothermal behavior of a brick cavity wall: part B

Karagiozis, Achilles; Salonvaara, Mikael

https://doi.org/10.4224/20328782

IEA ANNEX 24 TASK 1 SIMPLIFIED MODELING

HYGROTHERMAL BEHAVIOR OF A BRICK CAVITY WALL

PART B

Parametric Study on Material Properties Using Stochastic Modeling

by Achilles Karagiozis & Mikael Salonvaara

Abstract

In contrast to energy transport, moisture transport directly impacts the basic porous structure of building envelope construction. A one-dimensional computer model is used to numerically analyze the effect of randomly altering the porous material transport properties, under cold climate conditions. The hourly hygrothermal performance of a brick layered cavity wall, as detailed in the sixth IEA Annex 24 exercise, was investigated using a randomly changing material structure. A first order spatial stochastic random walk method was implemented in the LATENITE model. Two independent tests were investigated, one where the stochastic processes requiring both the means and the variances of each investigated transport property varying simultaneously every time step, and the other once in the beginning of each simulation. A Monte Carlo method was used to generate the uniform probability density functions of each investigated transport property by a controlled variation of ± 40 %. Irrespective of the two stochastic procedures, the results show minor influences of the total moisture temporal distribution and the heat flux distribution. Maximum differences in yearly averaged heat losses for both stochastic methods fall under 7 %. The general conclusion is that the ± 40 % level of randomly varying material properties for this brick layered cavity wall did not produce major differences in the hygrothermal performance of this building envelope system. This implies the accuracy of the properties around the functional forms for transport properties may not be critically important. As an outcome some transport properties may be simplified allowing one to implement simplified modeling.

Introduction

The knowledge of the hygrothermal performance of building envelopes is critical early on during the conceptualization stage of each construction design. Moisture transport has been identified as one of the main reasons for building envelope deterioration in North America and Europe. These moisture damage problems are usually the outcome of a combination of unfortunate circumstances and design flaws. Albeit this, to date only a handful of hygrothermal models are available that integrate all important transport physics. Most of these models, reference (2) for details, are research tools requiring an enormous entry level of information. The distribution of these models to building designers are impede for two main reasons, first the large computational time required for simulation on today's friendly PC environment and second the sophistication of the input parameters, functional forms for the moisture transport properties, diffusivities and permeability, thermal properties and the weather conditions being the ambient temperature, relative humidity, solar radiation, wind speed, wind direction and rain precipitation. Simplification of the entry level of information becomes imperative in-order for building designers and architects to use HAMTIE models. In a recent paper, Ref. (3), the authors investigated the influence of the accuracy/reliability of the inputted material properties on the predictive capability of the hygrothermal simulation results. Results showed that a uniform simultaneous variation of ± 25 % in both vapor permeability and liquid diffusivity respectively of all materials in the wall system produced no significant differences in temporal moisture accumulation.

This present paper is a supplement to (1) (PART A), where the effect of simplification of the material properties was investigated by using three different functional forms ranging from the most complex to just constant properties through-out the analysis. An inherit assumption in PART A of the simulations, were that homogeneous time invariant material properties were employed. In those simulations material properties of each material in the brick layered cavity wall were assumed deterministic. However, in most construction materials, no two are alike. In addition most materials have great variances in both pore size, and pore distributions even within the same manufactured batch. Hence, in-order to determine whether a potential for simplified modeling exists, a sophisticated stochastic/Monte-Carlo module was implemented in the LATENITE hygrothermal model (4), (5) and (6). The LATENITE state of the art computer model was chosen for the simulations due to its open concept modular formulation. One dimensional simulations were carried out in this investigation.

Stochastic Monte Carlo Simulations

From a fundamental point of view heat and mass transfer mechanisms and, therefore, their effective properties are strongly related to the packing pattern of the porous media as well as to the mechanical and thermal properties of each substance. Due to the random nature of the packed bed system, there are no analytical or deterministic solutions to heat and mass transfer problems in porous media in a strict sense. A probabilistic method, the Monte Carlo technique, can be used to generate the material properties that occur during moisture transport.

This technique can be used to randomize the partial differential equations that describe heat and mass transfer through the porous media. This randomization must be constraint to satisfy conservation principles at all times. Solving a large number of these equations for each time step allows the methods to be extended to what is referred in this paper as quasi stochastic modeling. The implementation of this method for hygrothermal modeling allows a very broad parametric study to be conducted with minimal computational effort. Following is a brief introduction to the implemented method.

Theory

Monte Carlo has been defined as a technique of solving a problem by putting random numbers and getting out random answers. The answer for the problem is the average value of the random answers obtained. The basic concept of the Monte Carlo method is the random walk process, also termed the Markov chain. A Markov chain is simply a chain of events occurring in sequence. The probability of each succeeding event in the chain is uninfluenced by prior events. It is important to note the independence of each event in the sequence. To understand some of the very basic aspects of the method, we have chosen to describe here vapor transport by simple diffusion process.

Lets assume that the vapor molecules are homogeneous, (not necessary the media), meaning that the number density of the molecules per unit volume is uniform. Suppose that some molecules are labeled somehow (e.g. Canadians) but are otherwise identical to all the other unlabelled (e.g. Finnish) molecules. In equilibrium, the number density n(x,t) of the labeled molecules must also be uniform. If there is an excess concentration of the Canadian vapor molecules at some position x, there must be a deficit of Finnish molecules at x in order to keep the total number density uniform. In such a situation the Canadian molecules will move about as to make the vapor concentration more uniform. If Γ denotes the flux of Canadian vapor molecules crossing the point x and D the diffusion coefficient, then

$$\Gamma = -D\frac{\partial n}{\partial x}$$

Since the number of Canadian vapor molecules must be conserved, the continuity equation is

$$\frac{\partial n}{\partial t} = -\frac{\partial \Gamma}{\partial x}$$ and therefore

$$\frac{\partial n}{\partial t} = D\frac{\partial^2 n}{\partial x^2}$$

The solution of these equation can be written as,

$$n(x,t) = Np(x,t)$$ where,

$$p(x,t) = \frac{e^{-x^2/4Dt}}{(2\pi Dt)^{1/2}}$$

N is defined as the total number of Canadian vapor molecules. p(x,t) is interpreted as the probability that a Canadian molecule found at x=0 at t=0 will be found between x and x+dx at time t. For example, a normal probability density function is depicted in Figure (1).

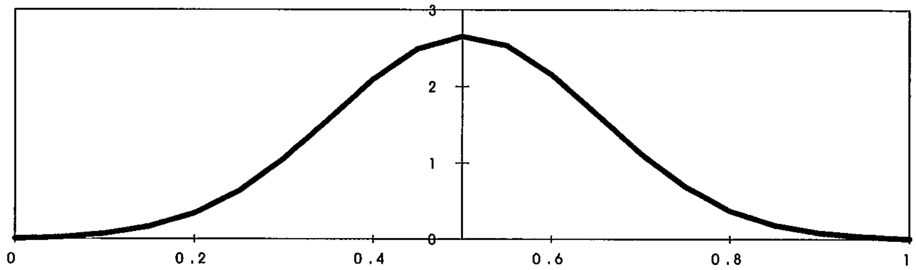

Figure 1 : Normal Probability Distribution

The mean square displacement at time t can be calculated as

$$\langle x^2 \rangle = \int_0^{\infty} x^2 p(x,t)\,dx = 2Dt$$

the diffusion coefficient can be written then as

$$D = \langle x^2 \rangle / 2t$$

The diffusion of the molecules may be considered as a random walk. Consider one Canadian vapor molecules initially at x=0. It has the same thermal velocity and travels straight line segments between collisions with the Finnish molecules. After each collision, it has an equal but random chance of moving to the right or left. The probability of being between x and x+dx after M steps of equal length b is

$$P(x,M)dx = \frac{e^{-x^2/2Mb}}{2\pi Mb^2}dx$$

Many other techniques concerning the Monte Carlo method are available in literature. The above merely shows basic principle and procedure of the method. It is important to note that the effective application of the Monte Carlo simulation technique depends on two important factors: the extent of knowledge of the process under study (HAMTIE EQUATIONS), qualitatively, and the amount of data available (quantitative). Knowledge of the process refers to the level of understanding of its behavior and characteristics.

IMPLEMENTATION

The relation of the differential equations describing the heat transfer and a simple stochastic model describing this phenomena has been known for some time (1). The same governing differential equations imbedded in LATENITE were used, but allowing a probabilistic interpretation, i.e., if a random-walking factor is given at point (x,y) for each material property under investigation. The primary objective of this work was to the parametric investigation of material property influences, a uniform probability density function was sought. However, due to the limited number of simulations employed some skewness existed, this will be discussed further. For the present investigation δ_p vapor permeability, D_w liquid diffusivity and thermal conductivity λ was randomized with ± 40 % of the full correlation of the property; i.e. the complete functional dependence on moisture content is taken into account.

Simulation Cases

Two independent tests were investigated, one (Case 1) where the stochastic processes requiring both the means and the variances of each investigated transport property varying simultaneously every time step, and the other (Case 2) once in the beginning of each simulation. A Monte Carlo method was used to generate the probability factors for each investigated transport property in a controlled fashion allowing variations limited to ± 40 %. Ten yearly simulations were conducted for each test, twenty in total. Each test was allowed to be independent of each other.

Wall structure:

To determine the sensitivity to the moisture and heat transport properties on the heat and moisture transport of a high rise wall structure several simulations were performed. The high rise wall structure selected for the numerical analysis is shown in Figure (2). The wall is composed of the following layers starting from the exterior to interior, a 90 mm facade brick (LATENITE database: material number 13), a 120 mm glass fiber board (material number 5) and finally a 140 mm red brick (material number 14). The height of the wall is 1 m (1-dimensional simulations). This particular wall assembly has no vapor barrier.

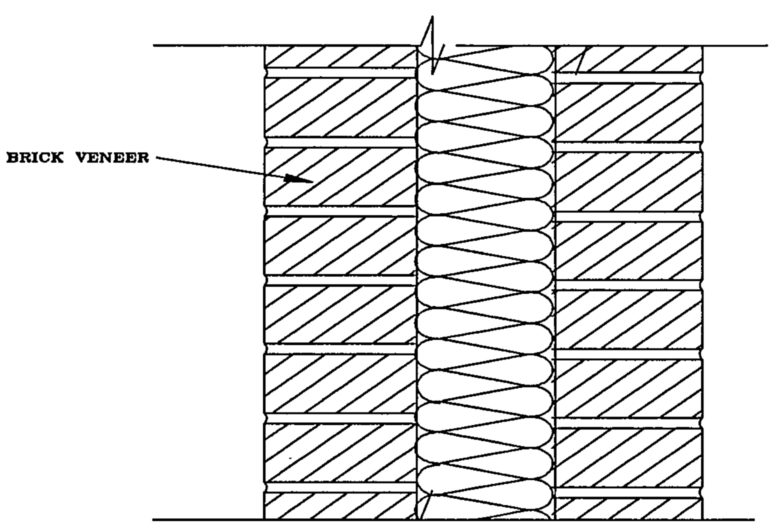

Figure 1. The analyzed wall structure.

The wall was exposed to outside air temperature, and the relative humidity varied according to the weather data from the selected location (Ottawa). The simulations were carried out for a one-year exposure and started from the 1 st of January. For each case, the liquid diffusivity, vapor permeability and thermal conductivity of the brick layers were varied randomly with a variance of ± 40 %. The properties of the glass fiber board remained constant throughout this investigation.

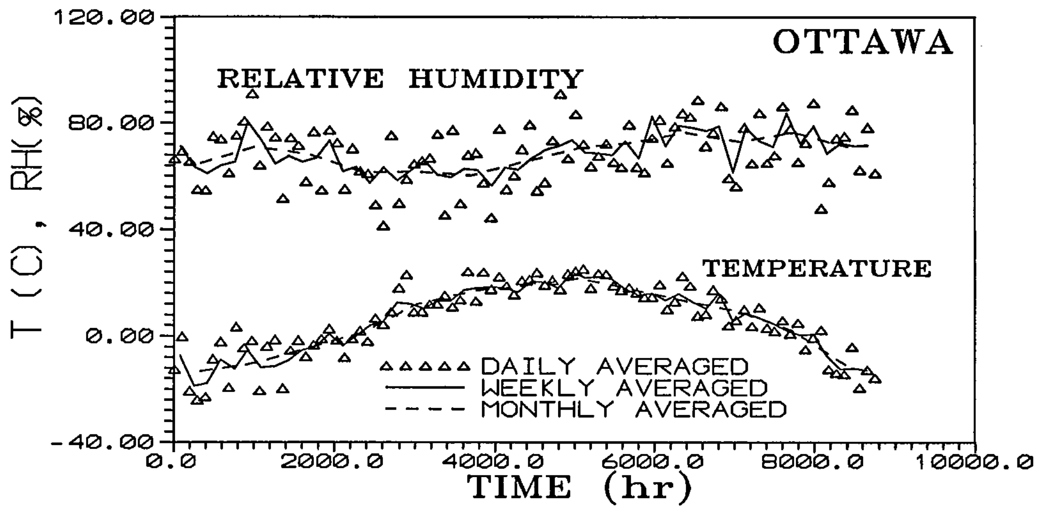

Figure 2 : Ottawa Weather Conditions for Daily, Weekly and Monthly Averaged Values

Boundary and initial conditions

Internal conditions were maintained constant at 21 °C and 40 % relative humidity (Pv= 997 Pa) throughout the 20 yearly simulations. The solar radiation and long wave radiation form the outer surfaces of the wall were included in the analysis. The BMY (Best Meteorological Year) weather file for the city of Ottawa was used. The daily, weekly and monthly averages of temperatures and relative humidities are plotted out in Figure 2. Figure 3 shows the daily, weekly and monthly averages of the solar fluxes on a south facing wall. The wall under consideration was centrally positioned on the third floor of a high rise building and was oriented facing North-West. All calculations started on the 1 st of January. Driving rain was used in the analysis as calculated by TASCflow. The additional moisture source due to direct incident of rain was also modeled. Inclusions of all these boundary conditions were considered in order to give the numerical analysis full credit in the sensitivity study. In this study no air infiltrating or exfiltrating is considered, thereby the primary mode of water transmission is due to diffusion processes.

The initial conditions of the wall were 10, 15 and 17 °C and 0.06, 0.009, 0.06 kg/kg moisture content for external brick, glass fiber and internal brick layer, respectively. The maximum capillary moisture content of the bricks is 0.111 kg/kg. Figure 4 plots out the moisture diffusivity employed for the internal brick. Here the ± 40 % maximum and minimum limits are shown for the Monte Carlo simulation.

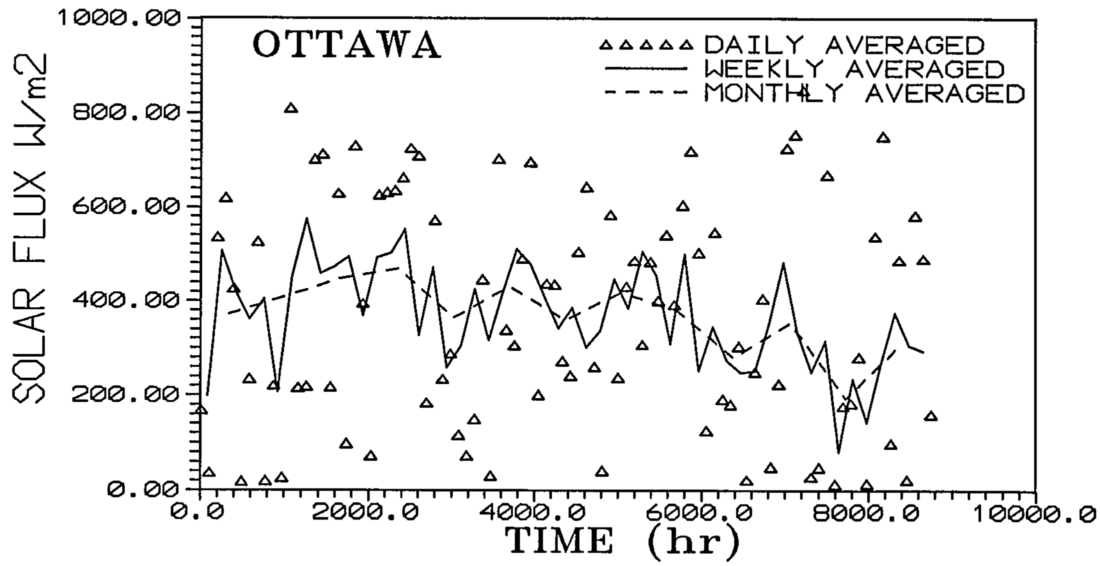

Figure 3 : Ottawa Solar Fluxes for Daily, Weekly and Monthly Averaged Values

The heat and mass transfer coefficients for external and internal surfaces are presented in Table 1.

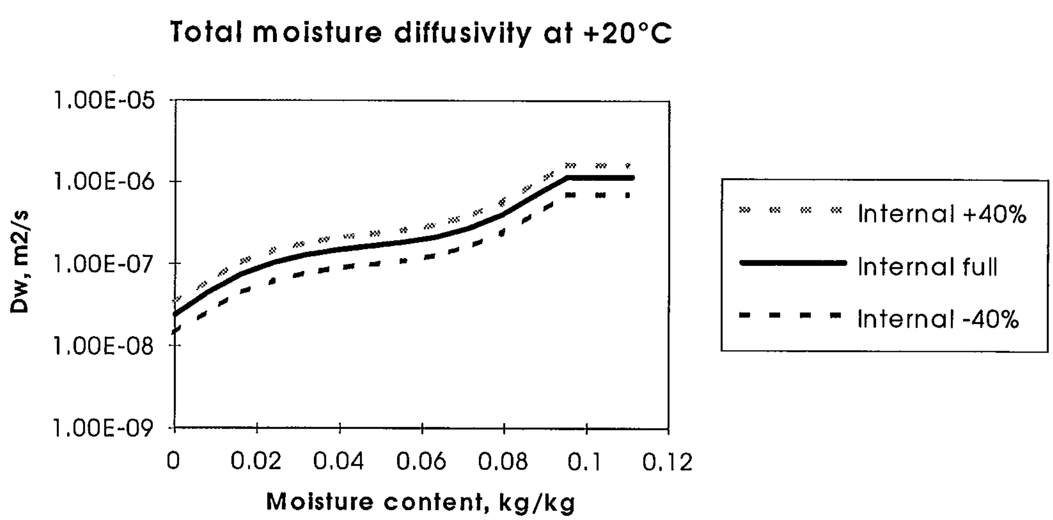

Figure 4 : Moisture Diffusivity Limits at ± 40 %

Table 1. Heat and moisture transfer coefficients for the external and internal surfaces.

Property	*External surface*	*Internal surface*
Heat transfer coefficients, W/ m^2K	20	8
Mass transfer coefficients, kg/m^2,s,Pa	$1.5 \cdot 10^{-7}$	$5.0 \cdot 10^{-8}$
Short wave absorptivity	0.6	-
Long wave emissivity	0.9	-

Results

Histograms

In Appendix 1 the frequency distributions along the cumulative behavior are shown for each of the runs of Case 2. Figures A1 to A10 demonstrate the randomness of each simulation. The y-label frequency is defined as the number of control volumes that have the same probability factor. The x-axis bins are arranged from values of 0.1 to 0.9, representing multiplication factors between 0.6 to 1.4, giving the -40 % and +40 % variation range for the material properties. These figures show the statistical distributions of the multiplication factor. Each of the 28 control volumes used had a randomly assigned multiplication factor and Figures A1 to A10 show the frequency of occurance for each simulation. As, an example in Figure A1 there are 3 control volumes at bin 0.1, and this corresponds to the multipication factor of 0.6. In Figure A11 all frequency histograms are summed up and the total frequency distribution is shown for Case 2. Here we can see that as the number of simulations enlarges, the probability density trend becomes the same (giving the same chance to each multiplication factor). In Figure A12, the relative frequency distribution and the normal is shown. It is clear that a normal distribution is not followed for these simulations.

Hygrothermal Results

In Appendix B, results on hygrothermal behavior of the brick-layered cavity wall are presented. The material properties for the interior and exterior brick were varied as shown in the Appendix A by ±40 %. Figure B1 depicts the relative humidity difference by daily averaging both Case 1 and Case 2 results. Results are shown for the control volume node closest to the interior of the external brick layer (node 10). The results show the maximum and minimum values as well as the actual relative humidity difference distribution for one simulation. Results clearly demonstrate that differences of up to ±40 % in material properties can cause differences in the order of 10 % in daily relative humidities. The hourly differences can be considerably higher up to 15 %. It is important to note that while a random ±40 % factor was used, the full functional form was followed. Figure B2 presents the maximum and minimum range results using Case1 and Case 2 stochastic approaches. It is evident that in Case 1 simulations, where the Monte Carlo simulations were carried out each time step, gave smaller differences with respect to the deterministic solution. Figure B3 shows the spatial relative humidity distribution after 225 days (mid August). Four curves are plotted out, one the deterministic solution, one from Case 1, and two from Case 2. The agreement observed between these different simulations, is indeed remarkable. This signifies that during that instant of time ±40 % differences in material properties have no effect on the hygrothermal performance of the wall. Figure B4 shows a similar plot but after a time period of 39 days (February). Here the deterministic and Case 2 simulations are compared, and differences of up to 14 % in relative humidities are present. Figures B5, B6 and B7 show the differences in total moisture between the deterministic and stochastic maximum and minimum values for both Cases 1 and 2. Figure B5 shows the full year results, while Figure B6 only the drying period and Figure B7 the remaining period. It becomes clear that with the exception of the drying period where the majority of the stochastic results dry faster, differences are small between the deterministic and stochastic results.

Figure B8 shows the maximum and minimum heat fluxes of all the stochastic runs. Results show very small influences, these primarily being the effect of the variation of the thermal properties of the interior and exterior brick. Most of these differences are present only during the drying and wetting seasons. Figure B9 shows the percentage differences in the yearly heat losses for Case 1 (first ten) and Case 2 (last ten). Maximum differences between the individual simulations and the average, are approximately 7 %.

CONCLUSIONS

Using the real (most complex) material property functions for material properties but randomly changing them by up to ±40 % produced local differences in relative humidities less than 15 %. Results further confirm PART A results that most of the differences exhibited arise from the effect of liquid diffusivities. The thermal performance is influenced mostly by the random changes in thermal conductivities.

Any differences in Case 1 and Case 2 simulation are attributed to differences in the probability density function employed in these cases. As the probability density function gives equal opportunity to each location, results deviate less from those determined by deterministic solutions.

The use of this quasi-stochastic approach allows a straightforward parametric investigation that provides important hygrothermal behavioral system information.

REFERENCES

1. Howell, J. R., Application of the Monte Carlo to Heat Transfer Problems, Advances in Heat Transfer, eds T.F. Irvine, Jr., and J.P. Harnett, vol. 5, pp 1-54, 1968
2. Hens, H. and Janssens A., "Inquiry on HAMCAT CODES", International Energy Agency, Heat, Air and Moisture Transfer in Insulated Envelope Parts, Report Annex 24, Task 1, Modeling, 1993.
3. Karagiozis, A. and Salonvaara, M, Influence of Material Properties on the Hygrothermal Performance of a High Rise Residential Wall, Accepted for ASHRAE 95 Symposium, Chicago, 1995
4. Karagiozis, A. "Overview of the 2-D Hygrothermal Heat-Moisture Transport Model LATENITE", Internal IRC/BPL Report, 1993.
5. Karagiozis, A. and Kumaran, K. Computer Models for Hygrothermal modeling of Building Envelopes, CFD Society of Canada, Montreal, June 1993.
6. Salonvaara M. and Karagiozis A., "Moisture Transport in Building Envelopes using an approximate Factorization Solution Method", CFD Society of Canada, Toronto, June 1-3 1994.
7. Hens, H. IEA, Annex 24, HAMTIE, First Common Exercise, Report number T1-B-91/05.
8. Kiessel, H. IEA, Annex 24, HAMTIE, Third Common Exercise, Holzkirchen 1993.
9. Beam, R. and Warming, R.: "An implicit factored scheme for the compressible Navier-Stokes Equations." *AIAA Journal*, Vol. **16**, No. 4, April 1978, pp. 393-402.

9\. Karagiozis A. and Salonvaara M., IEA Annex 24, First Common Exercise, Saskatoon, April 1992

APPENDIX A

SIMULATIONS FOR CASE 2

Figure A1. Frequency Histograms for Stochastic Simulation 1.

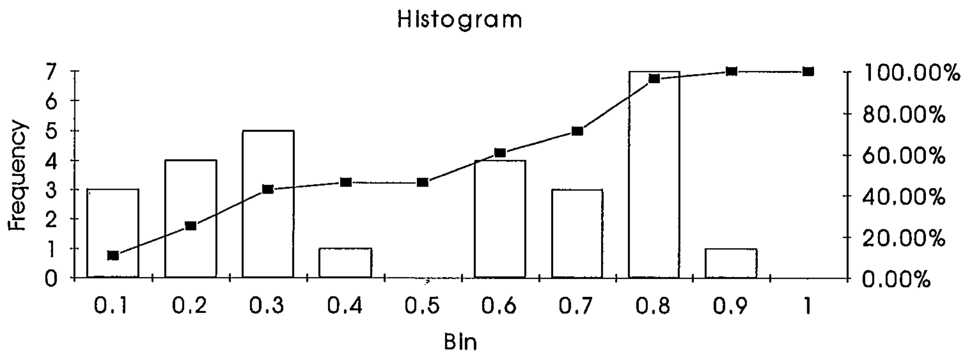

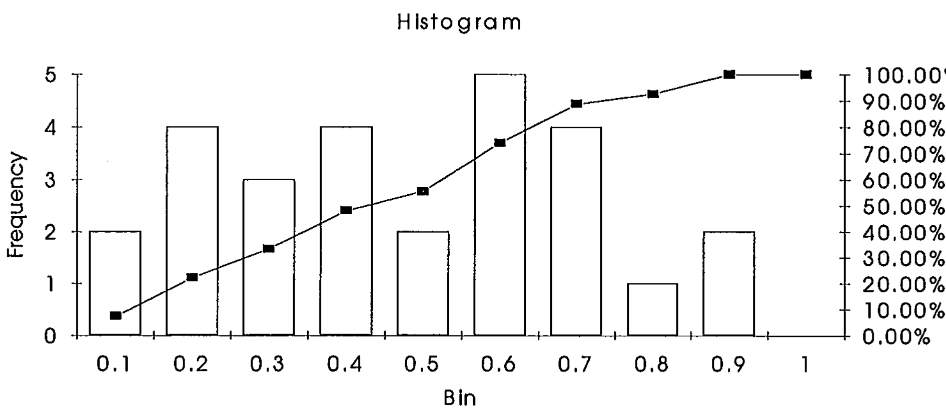

Figure A2. Frequency Histograms for Stochastic Simulation 2.

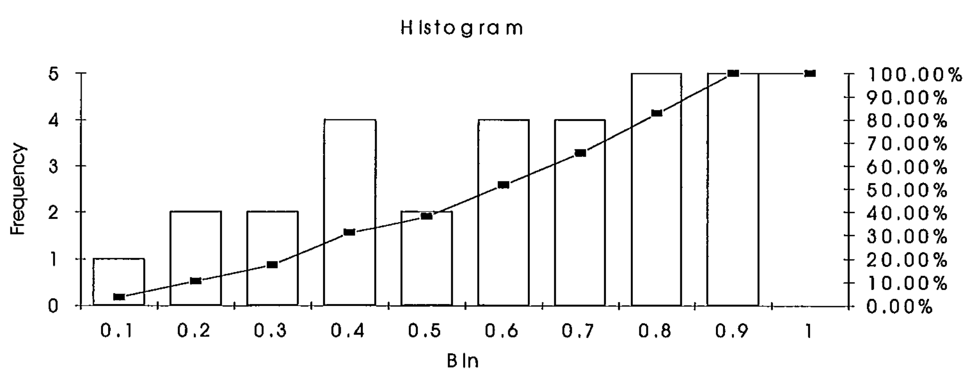

Figure A3. Frequency Histograms for Stochastic Simulation 3.

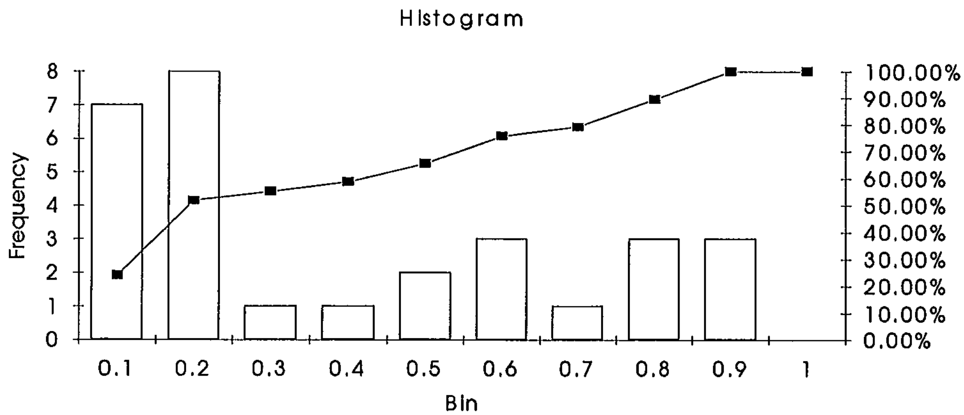

Figure A4. Frequency Histograms for Stochastic Simulation 4.

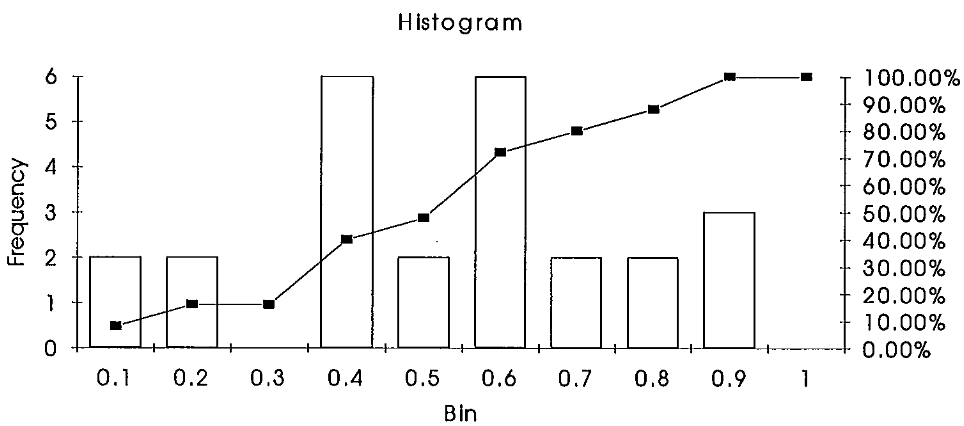

Figure A5. Frequency Histograms for Stochastic Simulation 5.

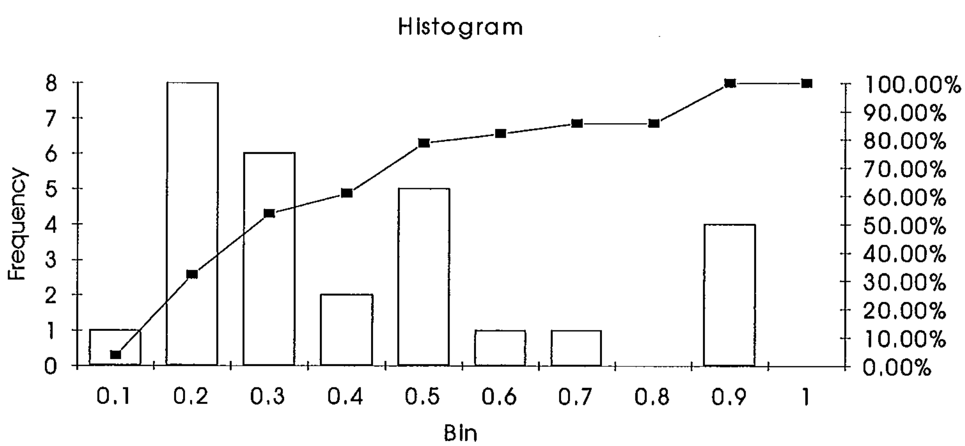

Figure A6. Frequency Histograms for Stochastic Simulation 6.

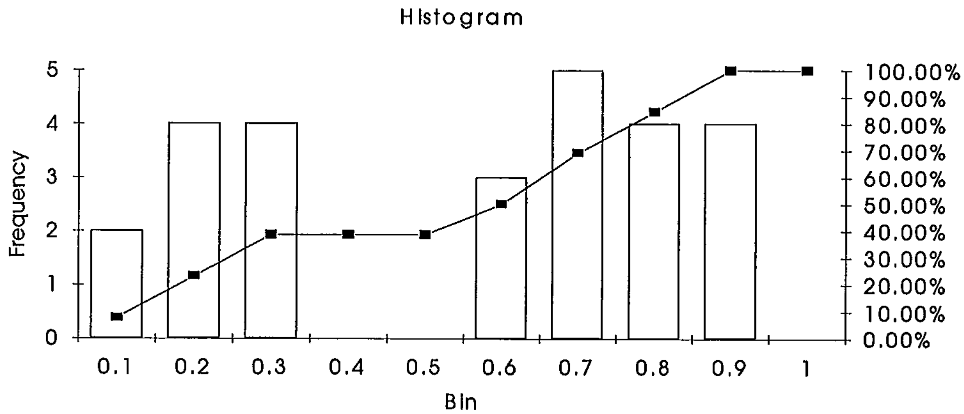

Figure A7. Frequency Histograms for Stochastic Simulation 7.

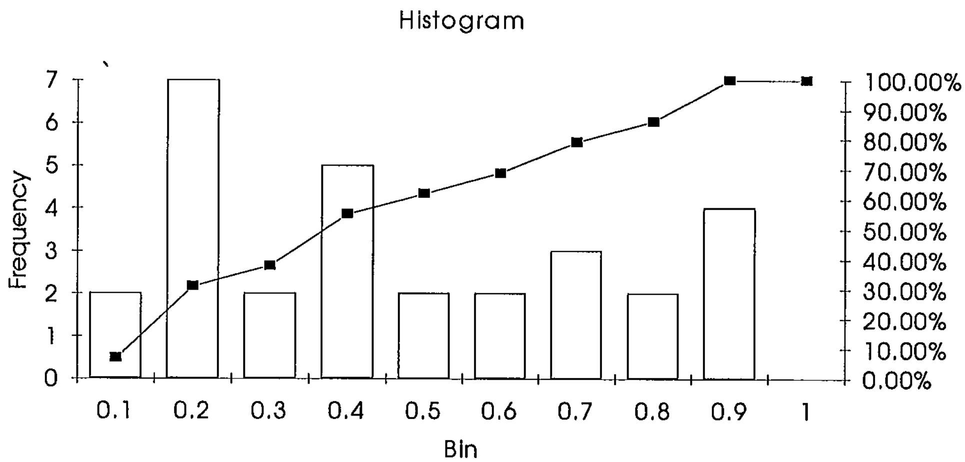

Figure A8. Frequency Histograms for Stochastic Simulation 8.

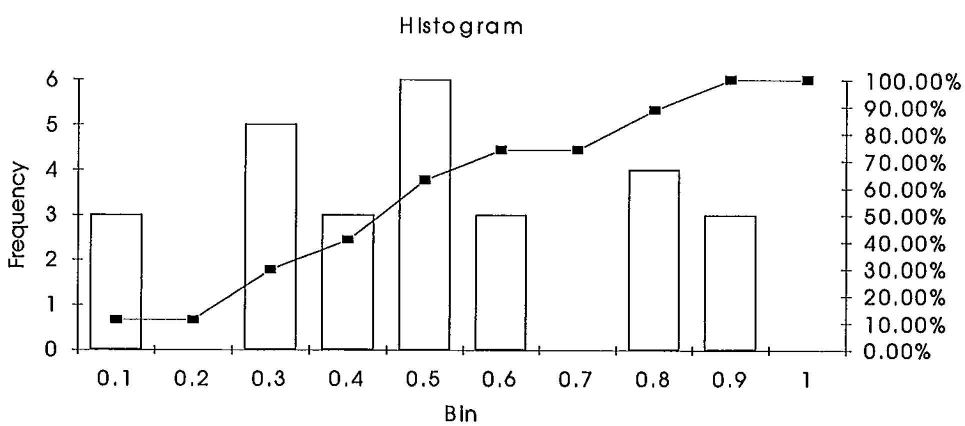

Figure A9. Frequency Histograms for Stochastic Simulation 9.

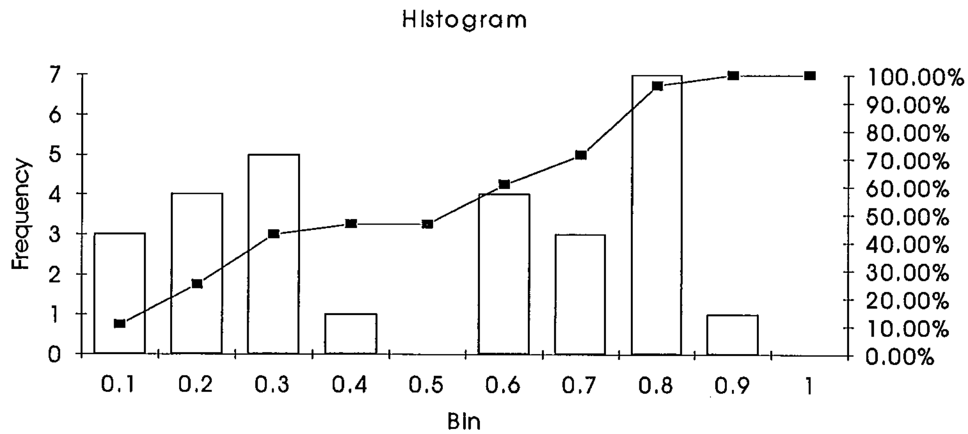

Figure A10. Frequency Histograms for Stochastic Simulation 10.

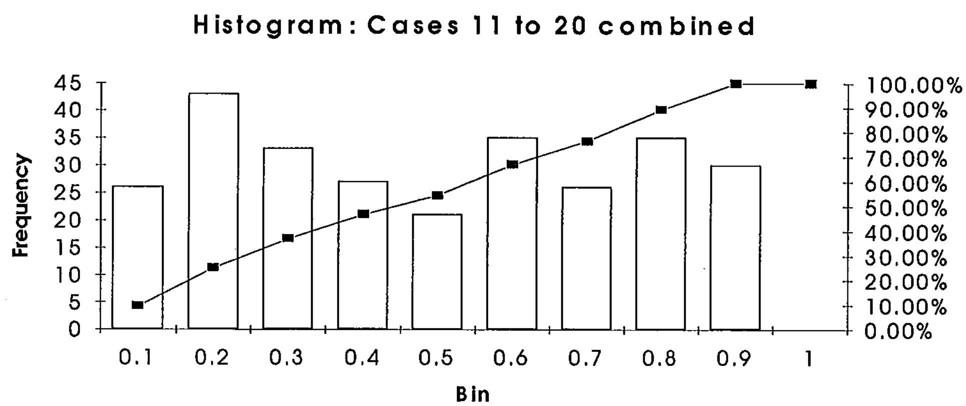

Figure A11. ***Combined Frequency Histograms for Stochastic Simulations 1-10 (Case 2).***

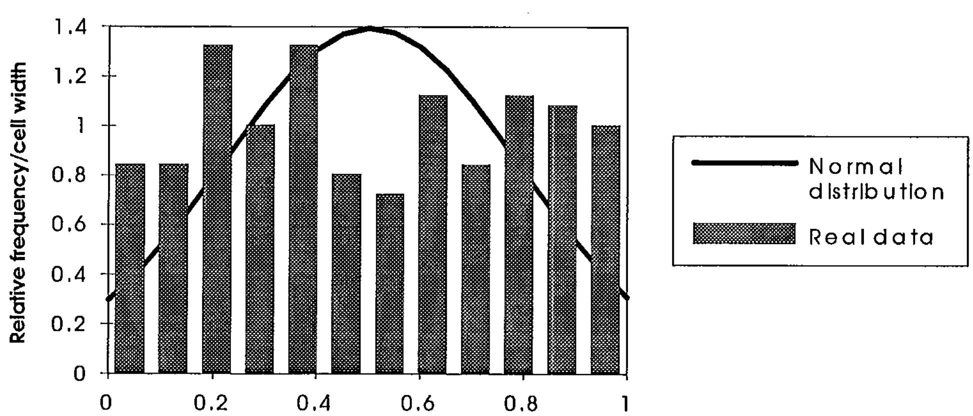

Figure A12. ***Real and Normal Probability Density Distributions for Stochastic Simulations 1-10 (Case 2).***

APPENDIX B

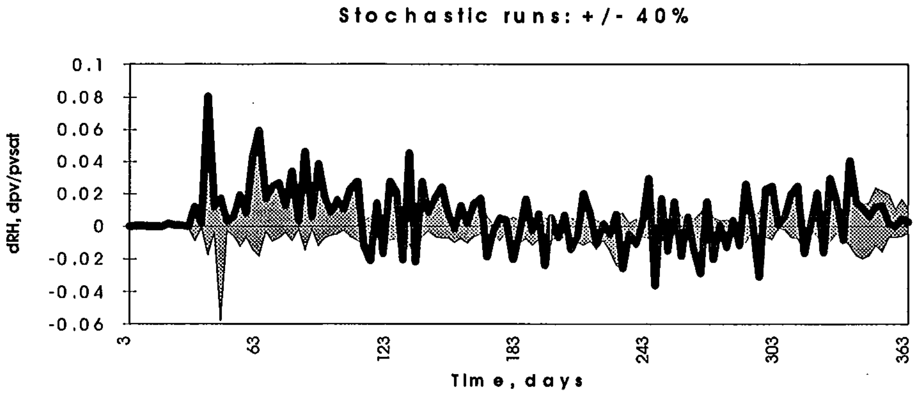

Figure B1. Relative humidity difference (daily averages) of the internal surface of external brick layer. Minimum and maximum variations and one of the 10 cases (solid line) are shown.

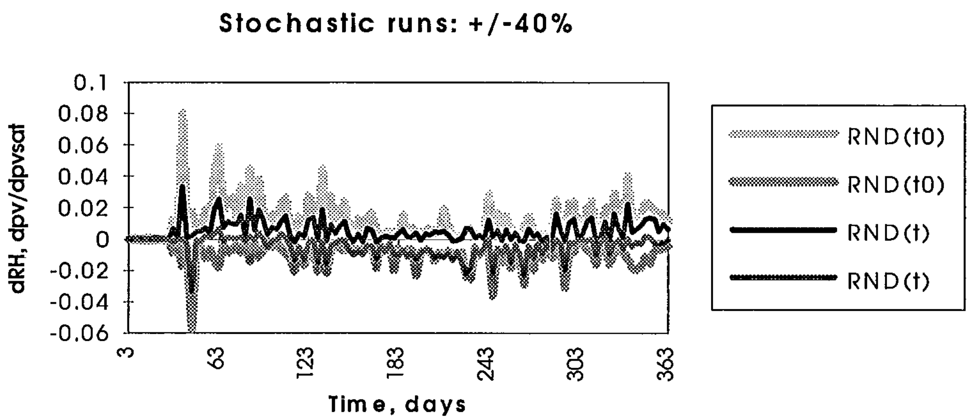

Figure B2. Relative humidity difference Comapring Case 1 (t) and Case 2 (t0) Simulations

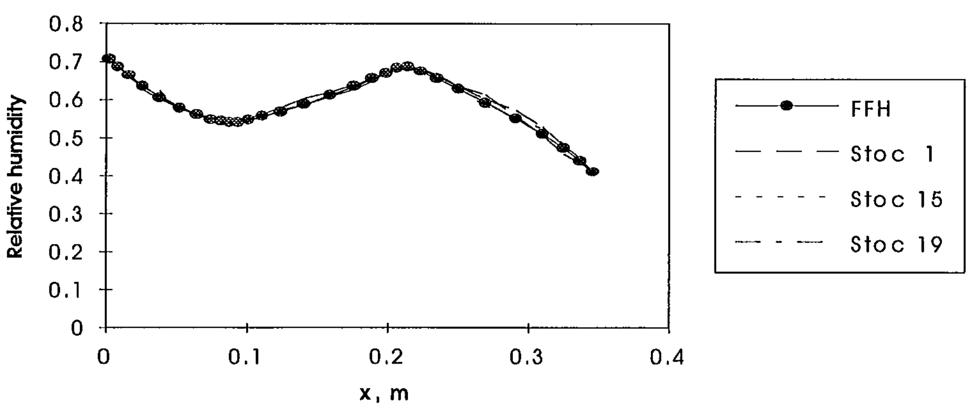

Figure B3. Comparison of Deterministic and Stochastic Simulations after 225 days≅ September

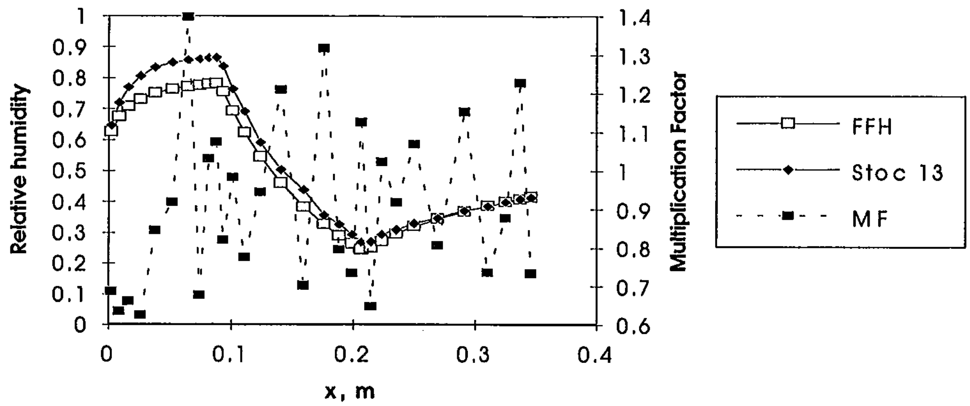

Figure B4. Comparison of Deterministic and Stochastic Simulations after 63 days≅ March

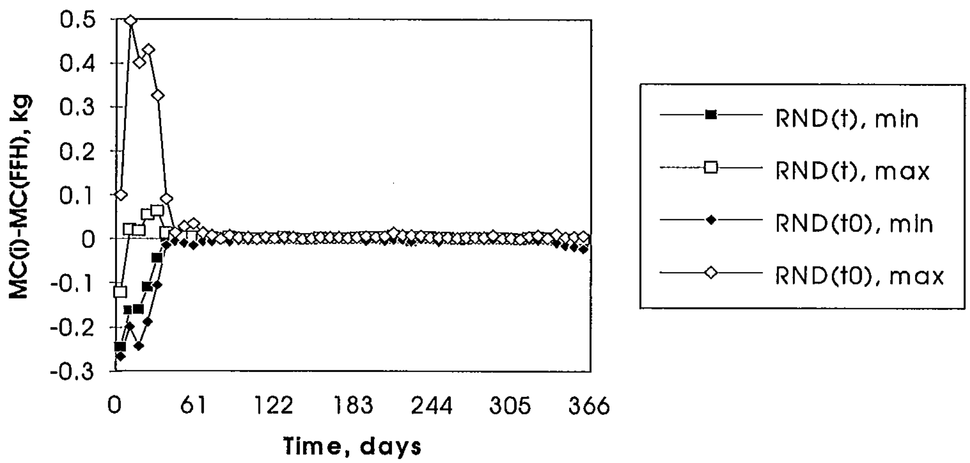

Figure B5. Total Moisture Differences between Stochastic Cases 1 and 2

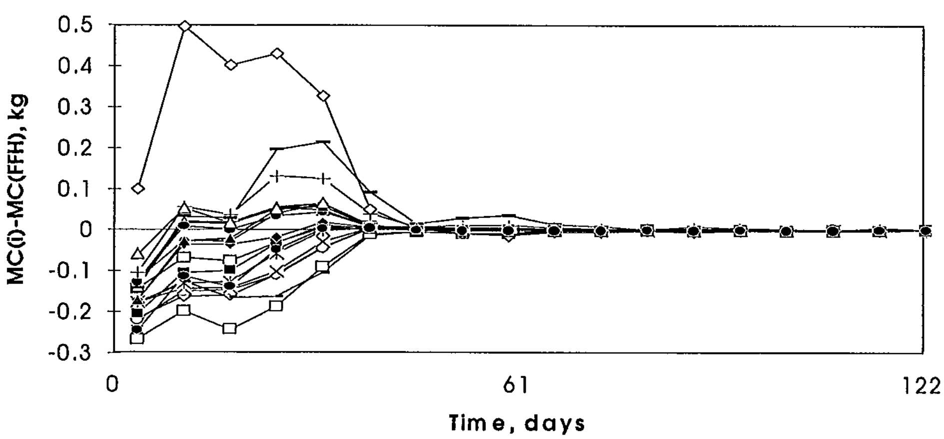

Figure B6. Total Moisture Differences between Stochastic Cases 1 and 2 during drying

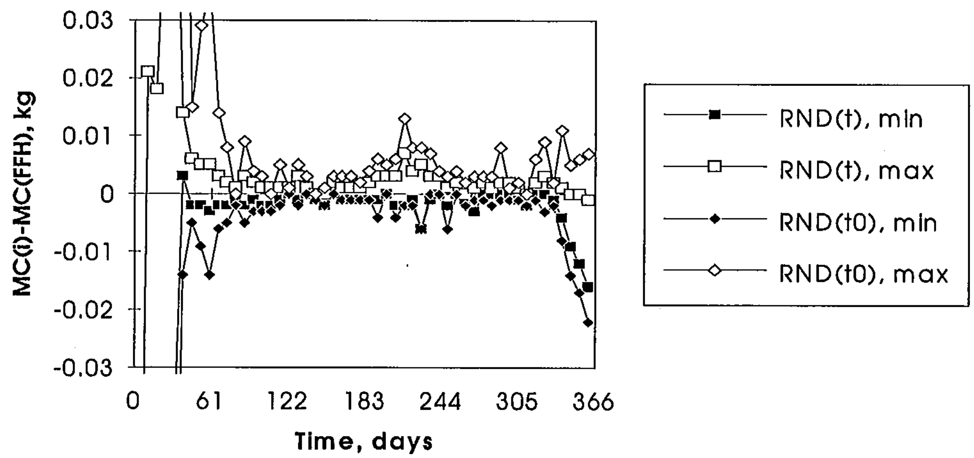

Figure B7. Total Moisture Differences between Stochastic Cases 1 and 2 after drying

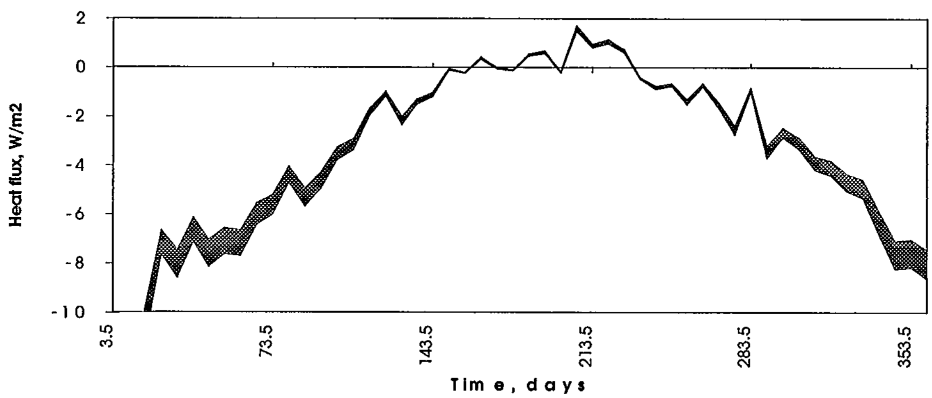

Figure B8. Minimum and maximum heat fluxes (daily averages) of all the stochastic runs

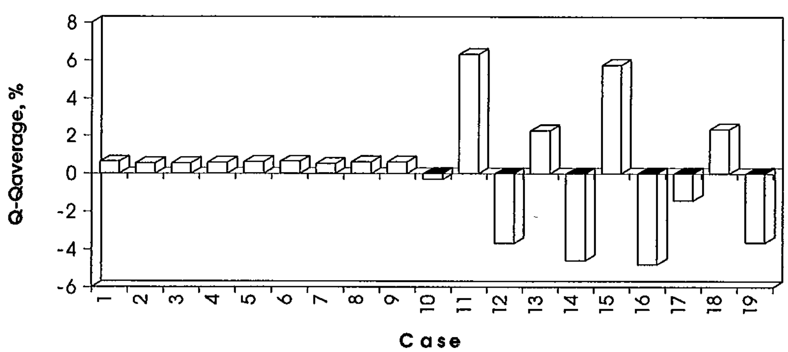

Figure B9. Differences in yearly average heat loss for stochastic runs. Material properties varied by ± 40%.